

# Optimal Guidance Law in the Plane

M. Guelman\*

*Laboratoire d'Automatique Théorique, Paris, France*  
and

J. Shinart†

*Technion, Haifa, Israel*

Using the exact nonlinear equations of motion in the plane, an optimal guidance law for a vehicle pursuing a maneuvering evader is derived. It is assumed that a complete knowledge of the evader's motion is available to the pursuer. Both the pursuer and the evader move with constant velocities. The guidance law minimizes a weighted linear combination of the time of capture and the expended maneuvering energy. The equations of motion are solved in closed form in terms of elliptic integrals. Numerical results are presented in order to illustrate the advantages of the optimal guidance law as compared both with proportional navigation and a trajectory formed by a hard turn followed by a straight line. The extension of the approach to the three-dimensional case is also outlined.

## I. Introduction

THE problem of deriving a feedback control law for a vehicle pursuing a maneuverable target has been of great interest for guided missile design. In many works, the analysis has been based on linearizing the pursuit geometry about a nominal collision course.<sup>1-5</sup> The linearization allows consideration of the time of pursuit as fixed. Using a quadratic index, the square of the "miss distance" at the fixed final time, plus the integral of a quadratic penalty on the control, the pursuit can be treated as a linear quadratic optimal control problem. Such analysis has demonstrated the optimality of the proportional navigation guidance law against a nonmaneuvering target.<sup>6,7</sup> A predetermined target maneuver can be treated similarly with the use of a modified guidance law.<sup>8,9</sup> Although linear control theory allows imposition of zero miss distance, it may require very large, sometimes infinite, controls. The above mentioned quadratic performance index provides a reasonable compromise which avoids excessive control expenditure.

The main drawback of the linearized approach is that the results apply only in a relatively small region of the state space, where the trajectory linearization is valid. This limitation prevails even if second-order terms are taken into account.<sup>10</sup>

In several other works, pursuit-evasion engagements have been analyzed, using the exact nonlinear equations of motion,<sup>11,12</sup> either as zero-sum differential games<sup>13</sup> or as one-sided optimal control problems.<sup>14</sup> If such mathematical models are used, the time of capture cannot be determined in advance. It has been shown,<sup>15</sup> however, that if the pursuer has higher speed and lateral acceleration than the evader as well as an ideal (instantaneous) control, there exists a control strategy that provides point capture (zero miss distance) at some finite time. Such analysis has assumed for simplicity constant speed vehicles, but the results apply for variable speed models also. The constant speed assumption can be justified by the fact that longitudinal accelerations of airborne vehicles are generally an order of magnitude lower than the lateral accelerations used for maneuvering.<sup>16</sup>

In many practical cases, it is of interest to minimize the time of capture even at the sacrifice of the point capture. This problem can be treated by formulating the capture criterion in terms of a fixed allowable miss distance. In order to avoid excessive control expenditure, adding a quadratic penalty integral to the performance index can be useful. Such a term can be interpreted for a constant speed model as the requirement for additional propellant to overcome the maneuver-induced drag.

The purpose of the present paper is to derive an optimal guidance law for the pursuing vehicle against a maneuvering target in a plane. It is assumed that perfect knowledge of the target motion is available to the pursuer. The optimality criterion is a weighted combination of the time of capture for a given miss distance and the expenditure of maneuvering energy. The analysis is based on the exact nonlinear equations of motion for constant speed vehicles.

## II. Problem Formulation

A pursuer  $P$  is attempting to capture an evader  $E$ . The vehicles have constant velocities  $V_P$  and  $V_E$ , respectively. The pursuer is able to control its normal acceleration  $u$ . The geometry of the planar pursuit is depicted in Fig. 1. The equations of motion are

$$\dot{\theta} = [V_P \sin(\theta - \gamma_P) - V_E \sin(\theta - \gamma_E)] / r, \quad \theta(0) = \theta_0 \quad (1)$$

$$\dot{r} = V_P \cos(\theta - \gamma_P) + V_E \cos(\theta - \gamma_E), \quad r(0) = r_0 \quad (2)$$

$$\dot{\gamma}_P = u / V_P, \quad \gamma_P(0) = 0 \quad (3)$$

where  $r$  is the relative distance between the two vehicles,  $\theta$  the line of sight direction, and  $\gamma_P$  and  $\gamma_E$  the pursuer and evader flight directions, respectively.  $\theta$ ,  $\gamma_P$ , and  $\gamma_E$  are all measured with respect to an inertial reference.  $\gamma_E = \gamma_E(t)$  is a given continuous function of time. The problem to be solved is to find a control  $u$  such that capture defined by

$$r(t_f) \leq R \quad (4)$$

is assured while the performance index  $J$

$$J = t_f + k \int_0^{t_f} u^2 dt \quad (5)$$

is minimized. In this formulation the maneuverability of the pursuer is not limited; however, the weighting factor  $k$  is

Received Aug. 11, 1980; revision received Nov. 28, 1983. Copyright © American Institute of Aeronautics and Astronautics, Inc., 1984. All rights reserved.

\*Currently Head, Department of Guidance and Control, Rafael, Ministry of Defence, Israel.

†Associate Professor, Department of Aeronautical Engineering, Associate Fellow AIAA.

selected in such a way that the required acceleration is realistic. It is assumed that the parameters of the problem ( $V_p$ ,  $V_E$ ,  $k$ ,  $R$ ) and the boundary conditions ( $r_o$ ,  $\theta_o$ ) are compatible with the capture condition in Eq. (4). Such a formulation leads to an unconstrained nonlinear optimization problem.

### III. Optimal Control Solution

We shall apply the maximum principle<sup>7</sup> to solve the optimization problem. Let us define an additional state variable  $\chi$  such that

$$\dot{\chi} = I + ku^2 \quad (6)$$

with  $\chi(0) = 0$ . Then

$$J = \chi_f \quad (7)$$

Let us now write the Hamiltonian for the system of Eqs. (1), (2), (3), and (7)

$$\begin{aligned} H = & \lambda_\theta [V_p \sin(\theta - \gamma_p) - V_E \sin(\theta - \gamma_E)] \\ & + \lambda_r [-V_p \cos(\theta - \gamma_p) + V_E \cos(\theta - \gamma_E)] \\ & + \lambda_\chi u/V_p + \lambda_\chi (I + ku^2) \end{aligned} \quad (8)$$

The adjoint variables are defined by the equations

$$\begin{aligned} \dot{\lambda}_\theta = & -\lambda_\theta [V_p \cos(\theta - \gamma_p) - V_E \cos(\theta - \gamma_E)]/r \\ & - \lambda_r [V_p \sin(\theta - \gamma_p) - V_E \sin(\theta - \gamma_E)] \end{aligned} \quad (9)$$

$$\dot{\lambda}_r = \lambda_\theta [V_p \sin(\theta - \gamma_p) - V_E \sin(\theta - \gamma_E)]/r^2 \quad (10)$$

$$\dot{\lambda}_\gamma = \lambda_\theta V_p \cos(\theta - \gamma_p)/r + \lambda_r V_p \sin(\theta - \gamma_p) \quad (11)$$

$$\dot{\lambda}_\chi = 0 \quad (12)$$

while their boundary values are derived from the transversality condition ( $\theta_f$  and  $\gamma_{pf}$  being assumed free):

$$\lambda_\theta(t_f) = 0 \quad (13)$$

$$\lambda_\gamma(t_f) = 0 \quad (14)$$

$$\lambda_\chi(t_f) = -I \quad (15)$$

$$\lambda_r(t_f) \text{ free} \quad (16)$$

Solving the adjoint system, Eqs. (9-16), along an optimal trajectory (see Appendix A) we find that the optimal control is obtained as a function of the current state vector and its final value. The result is

$$u^{*2} = V_p [\cos(\theta_f - \gamma_p) - \cos(\theta_f - \gamma_{pf})] / k\dot{r}_f \quad (17)$$

$$\text{sign}(u^*) = \text{sign}[\sin(\theta_f - \gamma_{pf})] \quad (18)$$

where

$$\dot{r}_f = V_E \cos(\theta_f - \gamma_E) - V_p \cos(\theta_f - \gamma_{pf}) \quad (19)$$

is the final relative velocity.

This optimal control law has the following geometrical interpretation. The numerator of Eq. (17) is the difference between the projections of the current and final pursuer velocity vectors on the terminal line of sight (LOS) as shown in Fig. 2. Since  $\dot{r}_f < 0$ , Eq. (17) implies that the projection of the final pursuer velocity on the terminal LOS attains its maximum value at the pursuit end. From Eq. (18), it follows that the control  $u^*$  steers the vector  $V_p$  towards this final

LOS. Equation (17) can be expressed as

$$u^{*2} = \frac{\epsilon}{k} \quad (20)$$

where

$$\epsilon = [V_p \cos(\theta_f - \gamma_p) - V_p \cos(\theta_f - \gamma_{pf})] / \dot{r}_f \quad (21)$$

### IV. Control Law Application

The control law obtained in the previous section is only partially defined. The control amplitude and sign are given as functions not only of the current state variables, but also of their final values. Unless these final values are defined the control law cannot be applied. The problem to be solved now is thus to find the actual values of  $\theta_f$  and  $\gamma_{pf}$ . This requires the solution of the entire system of Eqs. (1-3) when  $u^*$  is defined by Eqs. (17-18). However, the control law defined by Eqs. (17-18) has a most striking characteristic. It depends on the current value of only one state variable,  $\gamma_p$ . The current values of the other two state variables  $r$  and  $\theta$ , relating the evader to the pursuer, do not appear in the expression found for  $u^*$ . It appears then that, formally at least, the pursuer's motion can be integrated *independently* of the evader's motion.

The pursuer's motion is defined for  $\sin(\theta_f - \gamma_{pf}) > 0$  by

$$\dot{X}_p = V_p \cos \gamma_p \quad (22)$$

$$\dot{Y}_p = V_p \sin \gamma_p \quad (23)$$

$$\dot{\gamma}_p = \frac{I}{c} \sqrt{\cos(\theta_f - \gamma_{pf}) - \cos(\theta_f - \gamma_p)} \quad (24)$$

where

$$c = \sqrt{V_p k (-\dot{r}_f)} \quad (25)$$

Integrating the system of Eqs. (22-24) from  $t=0$ ,  $\gamma_p(0)=0$ ,  $X_p(0)=0$ , and  $Y_p(0)=0$  to  $t=t_f$  and  $\gamma(t_f)=\gamma_{pf}$  we obtain (see Appendix B)

$$t_f = \sqrt{2}c [K(\cos \psi_f) - F(\alpha_f, \cos \psi_f)] \quad (26)$$

$$X_{pf} = V_p (A \cos \theta_f + B \sin \theta_f) \quad (27)$$

$$Y_{pf} = V_p (A \sin \theta_f - B \cos \theta_f) \quad (28)$$

where

$$A = t_f - 2\sqrt{2}c [E(\cos \psi_f) - E(\alpha_f, \cos \psi_f)] \quad (29)$$

$$B = 2c \sqrt{\cos(\theta_f - \gamma_{pf}) - \cos \theta_f} \quad (30)$$

and  $F$  is the elliptic integral and  $K$  the complete elliptic integral of the first kind,  $E$  and  $E$  are the elliptic and complete elliptic integrals of the second kind and

$$\psi = (\theta_f - \gamma_p)/2 \quad (31)$$

$$\psi_f = (\theta_f - \gamma_{pf})/2 \quad (32)$$

$$\alpha_f = \arcsin[\cos(\theta_f/2)/\cos \psi_f] \quad (33)$$

Since it is assumed that the evader's motion is perfectly known as a function of time, we have at  $t=t_f$  (see Fig. 3)

$$(X_{Ef} - X_{pf}) = R \cos \theta_f \quad (34)$$

$$(Y_{Ef} - Y_{pf}) = R \sin \theta_f \quad (35)$$

These two equations, together with Eqs. (26)-(28), provide the necessary conditions to determine  $\theta_f$  and  $\gamma_{pf}$ .

It should be noted that to perform the computation,  $c$ , defined by Eq. (25), remains to be determined. Due to the dependence of  $c$  on  $r_f$  and on  $\gamma_E(t_f)$ , Eq. (26) is, in fact, an implicit equation for  $t_f$ . That is, there are three implicit algebraic equations, Eqs. (26), (34), and (35), for three unknowns,  $t_f$ ,  $\theta_f$ , and  $\gamma_{Pf}$ .

Let us now summarize the guidance law application: the control amplitude is provided by Eq. (17), the control sign is defined by Eq. (18), and the required final values are obtained by solving the nonlinear system of algebraic Eqs. (26), (34), and (35).

## V. Computational Results

Numerical methods have been employed to demonstrate the advantages of the optimal guidance law (OGL). A comparison was first made with pure proportional navigation (PPN)<sup>12</sup> where

$$u = NV_P \dot{\theta} \quad (36)$$

and  $N$  is the navigation constant.

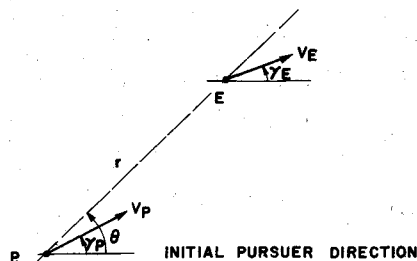


Fig. 1 Planar pursuit geometry.

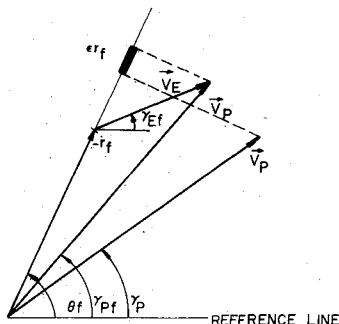


Fig. 2 Triangle of velocities.

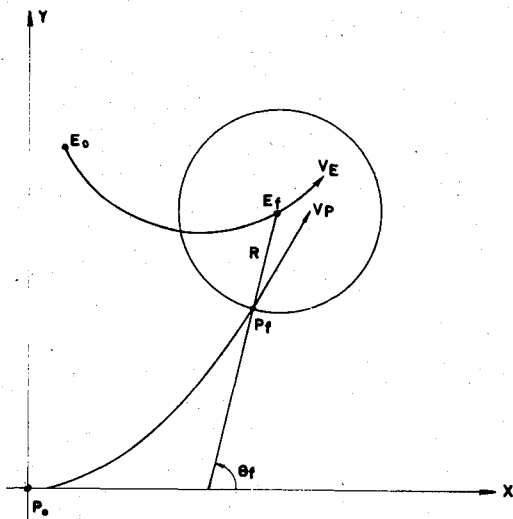


Fig. 3 Final interception geometry.

For comparison, an evader maneuvering with a constant turn rate  $\gamma_E^c$  was considered. In a first case the value of  $N$  in PPN was set equal to 4, the ratio of velocities,  $V_P/V_E$ , was equal to 2, and  $k = 10^{-4}$ . The trajectories are depicted in Fig. 4. It is seen that when the pursuer,  $P$ , employs PPN (the dashed trajectory) it is found to overreact at the beginning of the pursuit and is later obliged to change control direction due to the evader's maneuver. When employing OGL,  $P$  turns in only one direction. The final result is that with PPN,  $P$  captures the evader faster than with OGL, but the value of  $J$  is almost twice that obtained for OGL. Moreover, as can be seen in Fig. 5, where the normalized accelerations required by OGL and PPN are depicted as functions of time, the maximum acceleration required by PPN is almost four times the actual acceleration required by OGL.

In a second case, where  $V_P/V_E = 1.5$  and  $k = 10^{-4}$ , the trajectories are depicted in Fig. 6. The pursuer employing PPN (the dashed trajectory) starts with too small a value for the control ( $\dot{\theta}$  is small at departure) and consequently it has to increase the turning rate substantially later on in order to achieve capture. This maneuver takes a time which is almost twice as long as that required by OGL. From the normalized acceleration time histories depicted in Fig. 7 it can be observed that the PPN control changes sign twice during the pursuit and that the maximum required acceleration is almost twice the OGL requirement. These examples clearly show that OGL dramatically reduces the cost of the pursuit, and more importantly, reduces the maximum acceleration required in order to capture the evader.

Another comparison was made for the case in which  $P$  employs the strategy of a hard turn followed by a straight line path. This in fact is equivalent to the result of OGL for  $k \rightarrow 0$  (that is, the time optimal solution), with a hard limit on the control  $u$ , as can readily be seen from Eq. (17). When OGL is used, the sign of the control is determined by the final angular

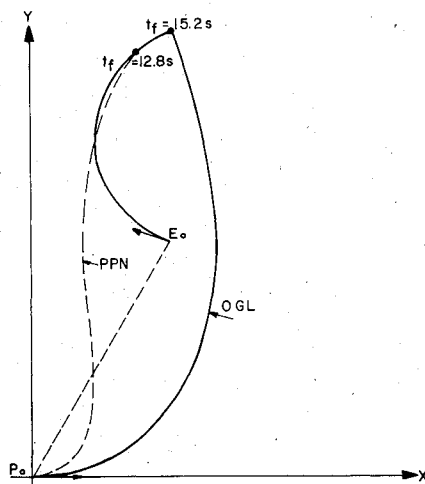


Fig. 4 Pursuer and evader trajectories,  $V_P/V_E = 2$ .

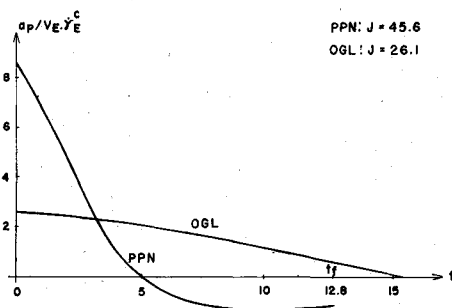


Fig. 5 Pursuer-evader acceleration ratio,  $V_P/V_E = 2$ .

values of the engagement, as defined in Eq. (18). For the simple hard turn strategy, the turn direction is not clear beforehand.

A simple solution to the hard turn strategy that does not require knowledge of the evader's trajectory, but only the current position, is to choose the turn direction to be the direction of the initial line of sight rotation. In many cases this can be an inefficient solution, as demonstrated in the present example. A hard turn is performed with  $u_{\max}^*$  a limit which is equal to the maximum value of the acceleration required by OGL with  $k = 10^{-4}$ , as shown in Fig. 7. It can be seen that on turning to the direction defined by the PPN at  $t = 0$ , a poor solution is obtained. Pursuit time is only slightly shorter than in the OGL solution, and a high penalty is paid for energy dissipation. When the right direction for the hard turn is selected, the time optimal solution is obtained, i.e., OGL with  $k = 0$ .

The two main advantages of the OGL are clear determination of the turn direction and the choice of the gain factor  $1/k$  which enables one to adapt the pursuer's trajectory to different pursuit conditions. For short ranges, where time is paramount,  $k \rightarrow 0$ ; for longer ranges, when maximum energy should be saved, a large  $k$  can be chosen.

For more benign cases, where the pursuer's initial conditions are such that trajectory is close to a collision course, the numerical results show that PPN behaves almost as well as OGL. This simply confirms previous theoretical results on the optimality of PPN when starting close enough to the collision course, in which case the trajectory linearization is still valid.

It should be noted that the usefulness of the OGL approach has been recognized, in spite of the adopted simplifying assumptions in the design phase of guided weapon systems.<sup>17</sup> Moreover, the approach can be easily extended to a three-dimensional engagement, as is discussed in the following section.

## VI. Extension to Three Dimensions

A complete three-dimensional analysis of the problem is clearly beyond the scope of the present paper. However, it is of interest to present briefly the results of a recent investigation<sup>18</sup> which indicate that the extension to the three-dimensional case is relatively straightforward.

Using three-dimensional vector notation, the equations of motion are written as

$$\dot{\mathbf{r}} = \mathbf{V}_E - \mathbf{V}_P, \quad \mathbf{r}(t_0) = \mathbf{r}_0, \quad |\mathbf{r}(t_f)| = R \quad (37)$$

$$\dot{\mathbf{V}}_P = \mathbf{a}_P \triangleq \omega_P \times \mathbf{V}_P, \quad \mathbf{V}_P(t_0) = \mathbf{V}_{P0} \quad (38)$$

where  $\mathbf{a}_P$  is the acceleration vector and  $\omega_P$  is the angular velocity vector for the pursuer.

Using the performance index, Eq. (5), with  $u = |\mathbf{a}_P|$ , the variational Hamiltonian is

$$H = -(1 + ku^2) + \lambda_r \cdot (\mathbf{V}_E - \mathbf{V}_P) + \lambda_v \cdot (\omega_P \times \mathbf{V}_P) \quad (39)$$

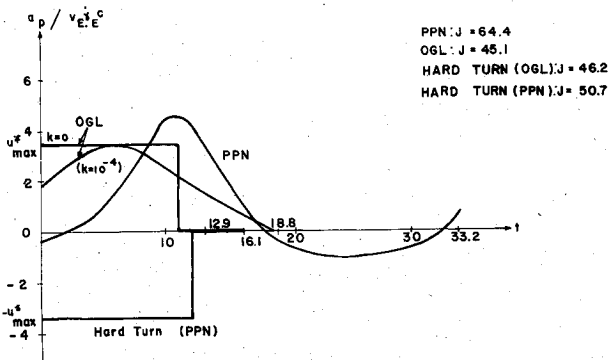


Fig. 6 Pursuer and evader trajectories,  $V_P/V_E = 1.5$ .

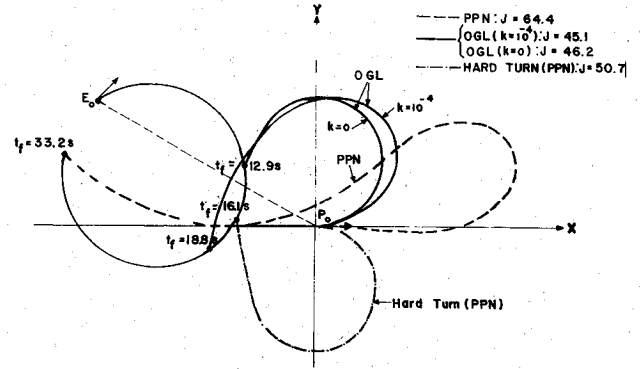


Fig. 7 Pursuer-evader acceleration ratio,  $V_P/V_E = 1.5$ .

The optimal control solution is expressed, in terms of acceleration amplitude, as

$$u^*(t) = \frac{1}{k} \{ 1 - \lambda_r(t) \cdot [\mathbf{V}_E(t) - \mathbf{V}_P(t)] \}^{1/2} \quad (40)$$

while the direction of the optimal acceleration vector  $\mathbf{a}_P^*$  is determined by

$$\mathbf{a}_P^*(t) \cdot [\lambda_v(t) \times \mathbf{V}_P(t)] = 0 \quad (41)$$

The last equation indicates that the vectors  $\mathbf{a}_P^*(t)$ ,  $\lambda_v(t)$ ,  $\mathbf{V}_P(t)$  are in the same plane.

Solution of the adjoint equation yields that

$$\lambda_r(t) = \lambda_r(t_f) = \nu \mathbf{r}(t_f) \quad (42)$$

where  $\nu$  is a scalar proportionality factor determined from the relation  $H^*(t_f) = 0$  as

$$\nu = 1 / (\mathbf{r}(t_f) \cdot [\mathbf{V}_E(t_f) - \mathbf{V}_P(t_f)]) \quad (43)$$

In addition

$$\lambda_v(t) \cdot [\mathbf{r}(t_f) \times \mathbf{V}_P(t_f)] = 0, \quad \forall 0 \leq t \leq t_f \quad (44)$$

which shows that  $\lambda_v(t)$  is confined to the plane determined by the vectors  $\mathbf{r}(t_f)$  and  $\mathbf{V}_P(t_f)$ . This plane is the terminal maneuver plane. The consequence of Eqs. (41) and (44) is that the instantaneous optimal maneuver plane defined by the vectors  $\mathbf{V}_P(t)$  and  $\mathbf{a}_P^*(t)$  coincides with the terminal maneuver plane.

Since the entire pursuer trajectory is confined to this plane, the solution presented in Sec. IV can be directly projected there.

## VII. Summary and Conclusions

The problem of finding a nonlinear optimal guidance law for a constant speed pursuing vehicle so as to capture a maneuvering target with a predetermined trajectory, while minimizing a weighted linear combination of time of capture and energy expenditure, has been solved in a closed form. The optimal control law is expressed as an explicit function of current and final values of the state variables. The closed-form solution of the equations of motion using this control law enables the determination of the required final states for guidance implementation. In a realistic environment, where the evader's trajectory is not known in advance, the application of the OGL has to be carried out step by step, based on real time estimation of the evader's current state and acceleration and the prediction of its future trajectory.

The merits of OGL as compared to other guidance strategies were demonstrated by a few numerical examples. It

was also shown that the planar analysis presented in the paper can be directly extended to three-dimensional engagements.

### Appendix A: Solution of the Adjoint Equations

From Eqs. (13) and (16)

$$\lambda_x = -' \quad (A1)$$

Rewriting Eqs. (10) and (11) and taking into account Eqs. (1) and (2)

$$\dot{\lambda}_\theta = \lambda_\theta \dot{r}/r - \lambda_r r \dot{\theta} \quad (A2)$$

$$\dot{\lambda}_r = \dot{\lambda}_\theta \dot{\theta}/r \quad (A3)$$

A solution for the system of Eqs. (46) and (47) of differential equations in terms of  $r$  and  $\theta$  is given by

$$\lambda_\theta = c_1 r \cos(\theta + c_2) \quad (A4)$$

$$\lambda_r = c_1 \sin(\theta + c_2) \quad (A5)$$

where  $c_1$  and  $c_2$  are constants of integration. This can be readily proved by direct substitution of Eqs. (A4) and (A5) into Eqs. (A3) and (A4). This solution was first pointed out in Ref. 13.

Substituting Eqs. (A4) and (A5) into Eq. (12) and rearranging yields

$$\dot{\lambda}_\gamma = c_1 V_p \cos(c_2 + \gamma_p) \quad (A6)$$

Substituting Eq. (18) into Eq. (3) yields

$$\dot{\gamma}_p = \lambda_\gamma / 2k V_p^2 \quad (A7)$$

From Eqs. (A6) and (A7), it follows that

$$\frac{d\lambda_\gamma}{d\gamma_p} = 2V_p^3 c_1 k \cos(c_2 + \gamma_p) / \lambda_\gamma \quad (A8)$$

Rearranging, integrating, and taking into account Eq. (15) yields

$$\lambda_\gamma^2 = 4V_p^3 c_1 k [\sin(c_2 + \gamma_p) - \sin(c_2 + \gamma_{pf})] \quad (A9)$$

We shall now find the values of  $c_1$  and  $c_2$ . At  $t = t_f$  Eqs. (4), (14), and (A4) imply that

$$c_1 R \cos(\theta_f + c_2) = 0 \quad (A10)$$

Thus

$$c_2 = \pi/2 - \theta_f + n\pi \quad (A11)$$

Due to the fact that we are dealing with a free end time problem, the Hamiltonian satisfies

$$H_f = 0 \quad (A12)$$

Taking into account Eqs. (14), (16), and (18), it follows that

$$H_f = \lambda_{r_f} \dot{r}_f - I = 0 \quad (A13)$$

where

$$\dot{r}_f = V_E \cos(\theta_f - \gamma_{E_f}) - V_p \cos(\theta_f - \gamma_{pf}) \quad (A14)$$

Recalling Eqs. (A11) and (A5) yields

$$H_f = \pm c_1 \dot{r}_f - I = 0 \quad (A15)$$

Thus

$$c_1 = \pm I / \dot{r}_f \quad (A16)$$

Substituting  $c_1$  and  $c_2$  into Eqs. (A4), (A5), and (A9) yields

$$\lambda_\theta = \frac{r}{\dot{r}_f} \sin(\theta_f - \theta) \quad (A17)$$

$$\lambda_r = \frac{I}{\dot{r}_f} \cos(\theta_f - \theta) \quad (A18)$$

$$\lambda_\gamma^2 = \frac{4kV_p^3}{\dot{r}_f} [\cos(\theta_f - \gamma_p) - \cos(\theta_f - \gamma_{pf})] \quad (A19)$$

### Appendix B: Solution of the Pursuer's Equations of Motion

In Eq. (24), the variables can be separated as

$$\frac{cd\gamma_p}{\sqrt{\cos(\theta_f - \gamma_{pf}) - \cos(\theta_f - \gamma_p)}} = dt \quad (B1)$$

Let

$$2\psi = \theta_f - \gamma_p \quad (B2)$$

and

$$2\psi_f = \theta_f - \gamma_{pf} \quad (B3)$$

Substituting Eqs. (B2) and (B3) into Eq. (B1) and performing a trigonometric transformation yields

$$\frac{-\sqrt{2}cad\psi}{\sqrt{a^2 \sin^2 \psi - 1}} = dt \quad (B4)$$

where

$$a = 1/\sin \psi_f, \quad a^2 > 1 \quad (B5)$$

The left side of Eq. (B4) is solvable in terms of elliptic integrals.<sup>19</sup> Integrating Eq. (B4) from  $t=0$ ,  $\gamma_p=0$  to  $t_f$ ,  $\gamma_{pf}$  we obtain

$$\sqrt{2}c[K(\cos \psi_f) - F(\alpha_f, \cos \psi_f)] = t_f \quad (B6)$$

where  $F$  is the elliptic integral and  $K$  the complete elliptic integral of the first kind.  $\alpha_f$  is given by

$$\alpha_f = \arcsin(\cos(\theta_f/2) \cos \psi_f) \quad (B7)$$

Dividing Eqs. (22) and (23) by Eq. (24), changing variables, and rearranging yields

$$dX_p = -\sqrt{2}caV_p \frac{\cos(\theta_f - 2\psi)}{\sqrt{a^2 \sin^2 \psi - 1}} d\psi \quad (B8)$$

$$dY_p = -\sqrt{2}caV_p \frac{\sin(\theta_f - 2\psi)}{\sqrt{a^2 \sin^2 \psi - 1}} d\psi \quad (B9)$$

The right sides of Eqs. (B8) and (B9) are solvable in terms of elliptic integrals. Integrating from the initial to the final conditions on both sides ( $X_{p0}=0$ ,  $Y_{p0}=0$ ) yields Eqs. (27) and (28).

### References

- <sup>1</sup>Bryson A.E. Jr., "Linear Feedback Solutions for Minimum Effort Interceptions, Rendezvous and Soft Landing," *AIAA Journal*, Vol. 3, Aug. 1965, pp. 1542-1544.
- <sup>2</sup>Willems G., "Optimal Controllers for Homing Missiles," Rept. No. RE-TR-68-15, U.S. Army Missile Command, Redstone Arsenal, Alabama, Sept. 1968.

<sup>3</sup>Cottrell, R.G., "Optimal Intercept Guidance for Short-Range Tactical Missiles," *AIAA Journal*, Vol. 9, July 1971, pp. 1414-1415.

<sup>4</sup>Anderson, G.M., "Effects of Performance Index/Constraint Combinations on Optimal Guidance Laws for Air-to-Air Missiles," *Proceedings of NAECON*, Institute of Electrical and Electronic Engineers, May 1979, pp. 765-771.

<sup>5</sup>Anderson, G.M., "Comparison of Optimal Control and Differential Game Intercept Missile Guidance Laws," *Journal of Guidance and Control*, Vol. 4, March-April 1981, pp. 109-115.

<sup>6</sup>Kreindler, E., "Optimality of Proportional Navigation," *AIAA Journal*, Vol. 11, June 1973, pp. 878-880.

<sup>7</sup>Bryson, A.E. and Ho, Y.C., *Applied Optimal Control*, Blaisdell Publishing Company, Waltham, Mass., 1969.

<sup>8</sup>Asher, R.B. and Matuzewski, J.M., "Optimal Guidance for Maneuvering Targets," *Journal of Spacecraft and Rockets*, March 1974, pp. 204-206.

<sup>9</sup>Nasaroff, G.J., "An Optimal Terminal Guidance Law," *IEEE Transactions on Automatic Control*, June 1976, pp. 407-408.

<sup>10</sup>Axelband, E.Z., Hardy, F.W., "Quasi Optimal Proportional Navigation," *IEEE Transactions on Automatic Control*, Vol. A1-15, Dec. 1970, pp. 620-626.

<sup>11</sup>Guelman, M., "Qualitative Study of Proportional Navigation," *IEEE Transactions on Aerospace and Electronic Systems*, July 1971, pp. 337-343.

<sup>12</sup>Guelman, M., "The Closed Form Solution of Pure Proportional Navigation," *IEEE Transactions on Aerospace & Electronic Systems*, Vol. AES-12, July 1976, pp. 472-482.

<sup>13</sup>Simakova, E.N., "The Quality Problem in Pursuit Games for Inertial Systems," *Automation & Remote Control*, Vol. 35, Nov. 1974, pp. 1716-1724.

<sup>14</sup>Sridhar, B. and Gupta, N.K., "Missile Guidance Laws Based on Singular Perturbation Methodology," *Journal of Guidance and Control*, Vol. 3, April 1980, pp. 158-166.

<sup>15</sup>Cockayne, F., "Plane Pursuit with Curvature Constraints," *SIAM Journal of Applied Mathematics*, Vol. 15, Nov. 1967, pp. 1511-1516.

<sup>16</sup>Shinar, J. and Steinberg, D., "Analysis of Optimal Evasive Maneuvers Based on a Linearized Two-Dimensional Kinematic Model," *Journal of Aircraft*, Vol. 14, Aug. 1977, pp. 795-802.

<sup>17</sup>Mirande, M., Lemoine, M., and Dorey, E., "Application of Modern Control Theory to the Guidance of an Air to Air Dogfight Missile," AGARD Proceedings No. 292, Oct. 1980, pp. 21.1-21.12.

<sup>18</sup>Shinar, J., "On Three Dimensional Pursuit Evasion," TAE Rept. No. 507, Dept. of Aeronautical Engineering, Technion, Haifa, Israel, March 1983.

<sup>19</sup>Gradshteyn, I.S. and Ryzhik, I.M., *Table of Integrals, Series and Products*, Academic Press, 1965.

## *From the AIAA Progress in Astronautics and Aeronautics Series...*

### **ENTRY HEATING AND THERMAL PROTECTION—v. 69**

### **HEAT TRANSFER, THERMAL CONTROL, AND HEAT PIPES—v. 70**

*Edited by Walter B. Olstad, NASA Headquarters*

The era of space exploration and utilization that we are witnessing today could not have become reality without a host of evolutionary and even revolutionary advances in many technical areas. Thermophysics is certainly no exception. In fact, the interdisciplinary field of thermophysics plays a significant role in the life cycle of all space missions from launch, through operation in the space environment, to entry into the atmosphere of Earth or one of Earth's planetary neighbors. Thermal control has been and remains a prime design concern for all spacecraft. Although many noteworthy advances in thermal control technology can be cited, such as advanced thermal coatings, louvered space radiators, low-temperature phase-change material packages, heat pipes and thermal diodes, and computational thermal analysis techniques, new and more challenging problems continue to arise. The prospects are for increased, not diminished, demands on the skill and ingenuity of the thermal control engineer and for continued advancement in those fundamental discipline areas upon which he relies. It is hoped that these volumes will be useful references for those working in these fields who may wish to bring themselves up-to-date in the applications to spacecraft and a guide and inspiration to those who, in the future, will be faced with new and, as yet, unknown design challenges.

*Volume 69—361 pp., 6 × 9, illus., \$22.00 Mem., \$37.50 List*  
*Volume 70—393 pp., 6 × 9, illus., \$22.00 Mem., \$37.50 List*

TO ORDER WRITE: Publications Dept., AIAA, 1290 Avenue of the Americas, New York, N.Y. 10104